

# Photofunctionalization of Alginate Hydrogels to Promote Adhesion and Proliferation of Human Mesenchymal Stem Cells

Oju Jeon, PhD,<sup>1</sup> and Eben Alsberg, PhD<sup>1,2</sup>

Photocrosslinkable biomaterials are promising for biomedical applications, as they can be injected in a minimally invasive manner, crosslinked *in situ* to form hydrogels with cells and/or bioactive factors, and engineered to provide instructive signals to transplanted and host cells. Our group has previously reported on biodegradable, photocrosslinkable alginate (ALG) hydrogels with controlled cell adhesivity for tissue engineering. The polymer backbone of this methacrylated ALG was covalently modified with cell adhesion ligands containing the RGD sequence to enhance the proliferation and differentiation response of encapsulated cells. However, this approach permits limited control over the spatial presentation of these ligands within the three-dimensional hydrogel structure. Here we present a system that easily allows for spatial control of cell adhesion ligands within photocrosslinked ALG hydrogels. A cell adhesive peptide composed of the specific amino acid sequence Gly-Arg-Gly-Asp-Ser-Pro (GRGDSP) was covalently modified with acrylate moieties. The acrylated peptide was then covalently incorporated into bulk hydrogels by adding it to methacrylated ALG solutions with a photoinitiator, and then photocrosslinking under long-wave ultraviolet light. The hydrogels were characterized with respect to their swelling and degradation profiles, and the effects of the acrylated peptide on human mesenchymal stem cell (hMSC) viability, adhesion, spreading, and proliferation were examined *in vitro*. hMSC adhesion and spreading on and proliferation in this biomaterial system could be regulated by varying the concentration of cell adhesion ligand. This new biomaterial system may be a useful platform for tissue engineering, drug delivery, and stem cell transplantation with spatial control of cell adhesivity.

## Introduction

RECENTLY, WE HAVE developed a photocrosslinkable alginate (ALG) hydrogel system with controllable mechanical and degradation properties.<sup>1,2</sup> The photocrosslinked ALG hydrogels exhibit excellent cytocompatibility, and are promising as cell carriers for tissue engineering applications since macromer solutions containing cells or soluble drugs can be injected minimally invasively into the target tissue defect, and then rapidly transformed into hydrogels *in situ* by ultraviolet (UV) light. However, due to the strongly hydrophilic nature of ALG and resultant low serum protein adsorption, cells are unable to interact with the material via cell surface receptors.<sup>3,4</sup> Therefore, we have previously covalently modified the photocrosslinkable ALG with the cell adhesion ligands containing the Arg-Gly-Asp (RGD) amino acid sequence using standard carbodiimide chemistry to form a biodegradable, photocrosslinked ALG hydrogel with controlled cell adhesivity.<sup>5,6</sup> Conjugation with cell adhesion ligands (Gly-Arg-Gly-Asp-Ser-Pro [GRGDSP]) resulted in

increased attachment and spreading of cells on the surface of hydrogels as well as proliferation and glycosaminoglycan production by encapsulated chondrocytes. Although the addition of the RGD-containing ligands improved cellular function, this process of chemical modification requires purification steps that may induce peptide inactivation<sup>7</sup> to remove unwanted byproducts. In addition, peptide incorporation efficiency was quite low at 37.6%. Potentially more importantly, this method is not easily adapted for spatial control over or variation of the presentation of adhesion ligands within the hydrogel. Dilutions of ligand-modified macromer solutions with unmodified macromer may be used to change the bulk concentration of ligands in formed hydrogels,<sup>8</sup> but ligand spacing in these hydrogels formed with different dilutions is not conserved or uniform. Each time a new ligand or ligand concentration is needed, new hydrogel macromer must be synthesized using this approach.

Photofunctionalization of biomaterials has been extensively utilized to induce desired cell-material interactions,

Departments of <sup>1</sup>Biomedical Engineering and <sup>2</sup>Orthopaedic Surgery, Case Western Reserve University, Cleveland, Ohio.

and provides improved spatial control over physical and biochemical signals in the presence of incorporated cells and bioactive factors.<sup>9–12</sup> A number of studies have focused on the integration of cell adhesion proteins or peptides by photofunctionalization of photocrosslinkable hydrogels.<sup>13–17</sup> Specifically, acrylation of cell adhesion proteins or peptides permitted successful incorporation throughout bulk hydrogels or in three-dimensional (3D) patterns with spatial control and precisely defined geometry to guide cell adhesion, migration, proliferation, and differentiation.<sup>13,18–23</sup>

In this study, we present a biodegradable, photocrosslinked ALG hydrogel system with the ability to spatially control the presentation of cell adhesion ligands using acrylated GRGDSP (ACR-RGD). Solutions of methacrylated ALG and ACR-RGD are uniformly mixed together, and during the photopolymerization the RGD is covalently bound to the ALG via free radical polymerization, and thus, is chemically incorporated throughout the bulk of the hydrogels. The effect of ACR-RGD incorporation on the physical properties of ALG hydrogels compared to unmodified ALG hydrogels were tested by examining differences in elastic moduli, swelling ratios, and degradation rates over time. The effect of ACR-RGD on human mesenchymal stem cell (hMSC) adhesion, spreading, and proliferation in two and three-dimensions was also investigated.

## Materials and Methods

### *Synthesis of photocrosslinkable ALG and ACR-RGD*

Low molecular weight sodium ALG (37,000 g/mol) was prepared by irradiating Protanal<sup>®</sup> LF 20/40 (196,000 g/mol; generous gift from FMC Biopolymer, Philadelphia, PA) at a gamma dose of 5 Mrad. Methacrylated ALG at a theoretical methacrylation of 15% (9.54% actual) was prepared as previously reported.<sup>1</sup> ACR-RGD was prepared by dissolving 200 mg GRGDSP (Commonwealth Biotechnologies, Richmond, VA) amino acid peptide sequence in a 10 mL buffer solution (6.5 pH) of 195.2 mg 2-morpholinoethanesulfonic acid (0.1 M; Sigma, St. Louis, MO) and 175.4 mg NaCl (0.3 M; Fisher Scientific, Pittsburgh, PA) that was stored for 10 min at  $-20^{\circ}\text{C}$  to reach  $\sim 4^{\circ}\text{C}$ . About 114.9 mg acrylic acid N-hydroxysuccinimide ester (acrylic acid-NHS; Sigma) was then added to the solution and the reaction was maintained at  $4^{\circ}\text{C}$  overnight (mole ratio of GRGDSP:acrylic acid-NHS = 1:2). The solution was then poured into 100 mL acetone and left to stand until a precipitate formed. The precipitate was washed thrice with clean acetone and allowed to dry. Then, the precipitate was dissolved in ultra pure deionized water ( $\text{diH}_2\text{O}$ ) and filtered through a  $0.22\ \mu\text{m}$  sterile syringe filter. The solution was then frozen and lyophilized. To verify the acrylation of the GRGDSP, unmodified and ACR-RGD were dissolved in deuterium oxide (Sigma) and placed in separate NMR tubes. The  $^1\text{H}$ -NMR spectra of the samples were recorded on a Varian Unity-300 (300 MHz) NMR spectrometer (Varian, Inc., Palo Alto, CA) using 3-(trimethylsilyl)propionic-2,2,3,3- $\text{d}_4$  acid (Sigma) as an internal standard.

### *Photocrosslinking*

To fabricate photocrosslinked ACR-RGD containing ALG hydrogels (ACR-RGD-ALG) for characterization, ALG (0.2 g) was dissolved in 9.9 mL  $\text{diH}_2\text{O}$  or Dulbecco's modified Eagle

medium (DMEM; Sigma) with 0.05% w/v photoinitiator (Irgacure-2959; Sigma), and then 100  $\mu\text{L}$  of ACR-RGD (1 mg/mL in  $\text{diH}_2\text{O}$  or DMEM with 0.05% w/v photoinitiator) solution was added to the ALG solution. To fabricate photocrosslinked ALG hydrogels without ACR-RGD as a comparative group, ALG (0.2 g) was dissolved in 10 mL  $\text{diH}_2\text{O}$  or DMEM with 0.05% w/v Irgacure-2959. These solutions were placed between two glass plates separated by 0.75 mm spacers and photocrosslinked with 365 nm UV light (Model ENF-260C; Spectroline, Westbury, NY) at  $\sim 1\ \text{mW}/\text{cm}^2$  for 10 min to form the hydrogels. Photocrosslinked hydrogel disks were created using a 6 mm diameter biopsy punch and placed in the same solution with which they were formed (i.e.,  $\text{diH}_2\text{O}$  or DMEM) for gross morphology, mechanical testing, swelling, and/or degradation studies.

### *Mechanical testing*

The elastic moduli of the photocrosslinked ACR-RGD-ALG or ALG hydrogels formed in DMEM were determined by performing constant strain rate compression tests using a Rheometrics Solid Analyzer (RSAII; Rheometrics, Inc., Piscataway, NJ) equipped with a 10 N load cell. The photocrosslinked ACR-RGD-ALG or ALG hydrogel disks were prepared with DMEM as described above and maintained in DMEM at  $37^{\circ}\text{C}$ . The DMEM was replaced every week. At the predetermined time points, swollen hydrogel disks were punched once again to form 6 mm diameter disks, their thickness was measured using calipers, and uniaxial, unconfined compression tests were performed on the hydrogel disks at room temperature using a constant strain rate of 5%/s. Elastic moduli of photocrosslinked ALG hydrogels were determined from the slope of stress versus strain plots, limited to the linear first 5% strain of the plots ( $N=3$  for each condition).

### *Swelling and in vitro degradation of ACR-RGD-ALG hydrogels*

The photocrosslinked ACR-RGD-ALG or ALG hydrogel disks were lyophilized and initial dry weights ( $W_i$ ) were measured. Dried hydrogel samples originally formed in DMEM were immersed in 50 mL DMEM, and incubated at  $37^{\circ}\text{C}$  to reach equilibrium swelling state. The DMEM was replaced every week. Over the course of 56 days, samples were removed, and the swollen ( $W_s$ ) hydrogel sample weights were measured. The swelling ratio ( $Q$ ) was calculated by  $Q = W_s/W_i$  ( $N=3$  for each condition per time point). After weighing the swollen hydrogels, they were lyophilized and weighed ( $W_d$ ). The percent mass loss was calculated by  $(W_i - W_d)/W_i \times 100$  ( $N=3$  for each condition per time point).

### *hMSC culture on the ACR-RGD-ALG hydrogels*

The hMSCs were isolated from a bone marrow aspirate and cultured in the Skeletal Research Center Mesenchymal Stem Cell Facility as previously described.<sup>24</sup> Photocrosslinked hydrogel disks were formed with various concentrations of ACR-RGD (0, 5, 10, and 20 mg ACR-RGD/g ALG) and DMEM in 24-well tissue culture plates. hMSCs (passage number 2) were seeded onto the hydrogels in 1 mL DMEM containing 10% fetal bovine serum (FBS; Sigma) and 1% penicillin-streptomycin (MP Biomedicals, Inc., Solon,

OH) at a seeding density of  $10^4$  cells/cm<sup>2</sup> and allowed to adhere for 4 h in a humidified incubator at 37°C with 5% CO<sub>2</sub>. The photocrosslinked ACR-RGD-ALG or ALG hydrogel disks were then transferred to new 24-well plates containing fresh serum containing medium. The medium was replaced every 3 days. The viability and morphology of adhered hMSCs on the photocrosslinked hydrogels disks were examined using a Live/Dead assay comprised of fluorescein diacetate (FDA; Sigma) and ethidium bromide (EB; Sigma) ( $N=3$  for each condition per time point). FDA stains the cytoplasm of viable cells green, while EB stains the nuclei of nonviable cells orange-red. The staining solution was freshly prepared by mixing 1 mL of FDA solution (1.5 mg/mL of FDA in dimethyl sulfoxide [Research Organics, Inc., Cleveland, OH]) and 0.5 mL of EB solution (1 mg/mL of EB in phosphate buffered saline [PBS, pH 7.4]) with 0.3 mL of PBS (pH 8). At predetermined time points, 20  $\mu$ L of staining solution was added into each well and incubated for 3–5 min at room temperature in the dark, and then stained hydrogel-cell constructs were imaged using fluorescence microscopy (ECLIPSE TE 300; Nikon, Tokyo, Japan) and a digital camera (Retiga-SRV; Qimaging, Burnaby, Canada). For nuclear staining, samples were rinsed with PBS and fixed in 4% paraformaldehyde in PBS for 10 min. Fixed hMSCs were permeabilized with 0.1% Triton X-100 in PBS for 5 min, and washed twice with PBS. One hundred microliter of 4',6-diamidino-2-phenylindole (DAPI) solution (0.2  $\mu$ g/mL in PBS) was pipetted directly onto the hydrogel disks. After 30 min incubation in darkness at room temperature, samples were washed with PBS to remove unbound DAPI. The number of hMSC was quantified using three different fields of fluorescent microscopic images of DAPI stained nuclei for each disk ( $N=3$  for each condition per time point).

#### Photoencapsulation of hMSCs

hMSCs (passage number 2) were photoencapsulated in hydrogels with various concentrations of ACR-RGD (0, 5, 10, and 20 mg ACR-RGD/g ALG) by suspension in macromer solution (2% w/v in DMEM) with 0.05% w/v Irgacure-2959. The hMSC/macromer solutions ( $1 \times 10^6$  cells/mL) were pipetted (100  $\mu$ L) into 96-well tissue culture plates and photocrosslinked as described above. The hydrogel-hMSC constructs were removed from the wells, placed in 24-well tissue culture plates with 1 mL DMEM containing 10% FBS, and cultured for 28 days in a humidified incubator at 37°C with 5% CO<sub>2</sub>. The medium was replaced every 3 days. The viability of encapsulated hMSCs in the photocrosslinked RGD-modified ALG hydrogels was investigated using the Live/Dead assay ( $N=3$  for condition per time point). At each time point, samples were withdrawn from the serum containing medium and the DNA contents ( $N=6-10$  for each condition per time point) were measured as previous reported.<sup>5</sup> The DNA contents were calculated using a standard curve prepared from Calf Thymus DNA (Invitrogen, Carlsbad, CA) and normalized to the dry weights of the hydrogel-hMSC constructs.

#### Statistical analysis

All quantitative data is expressed as mean  $\pm$  standard deviation. Statistical analysis was performed with one-way analysis of variance with Tukey significant difference *post hoc*

test using Origin software (OriginLab Co., Northampton, MA). A value of  $p < 0.05$  was considered statistically significant.

## Results

### Characterization of ACR-RGD and photocrosslinked hydrogels

To incorporate adhesion ligands containing the RGD sequence into photocrosslinked ALG hydrogels during the photopolymerization process, the NHS-activated carboxylic acid group of acrylic acid was covalently coupled to the amines of GRGDSP peptides to form stable amide linkages (Fig. 1a). The <sup>1</sup>H-NMR spectra of ACR-RGD exhibit vinyl methylene protons (Fig. 1b, peaks labeled a, b, and b') that were newly formed by the reaction with acrylic acid-NHS, which are located at  $\delta 6.3$  and 5.8. The spectra demonstrate that the GRGDSP was successfully acrylated.

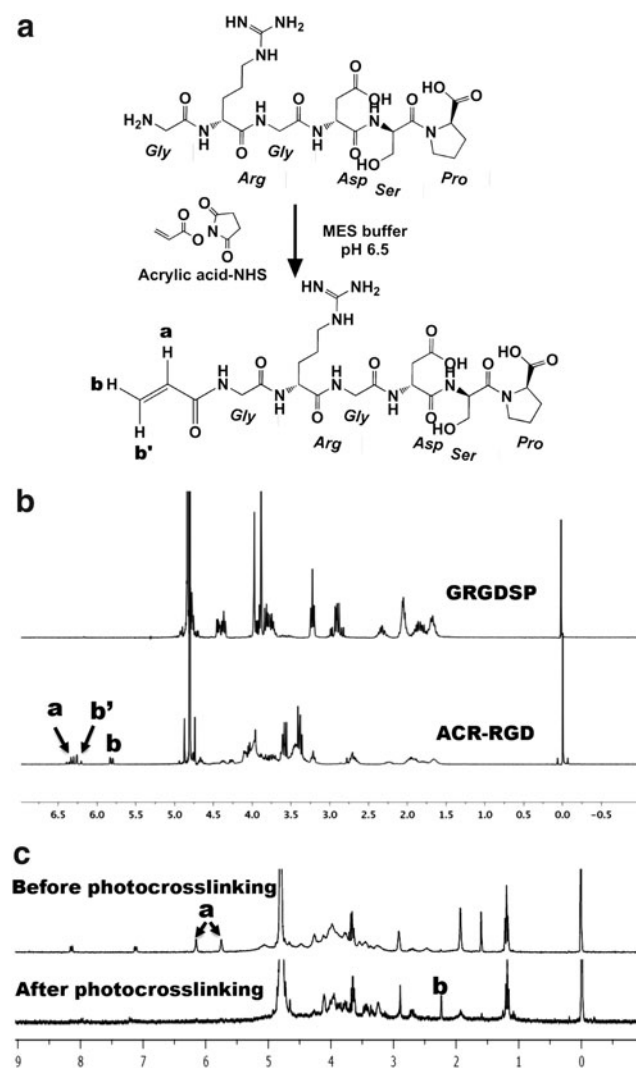


**FIG. 1.** (a) Schematic illustration of the Gly-Arg-Gly-Asp-Ser-Pro (GRGDSP) acrylation reaction, (b) <sup>1</sup>H-NMR spectra of the GRGDSP and ACR-RGD in D<sub>2</sub>O, and (c) <sup>1</sup>H-NMR spectra of ACR-RGD and alginate (ALG) before and after photocrosslinking together in D<sub>2</sub>O containing photoinitiator. (a, b', and c explained in Results section.)

The completeness of the photocrosslinking reaction between the methacrylated ALG and ACR-RGD was then verified with  $^1\text{H-NMR}$ . After photocrosslinking, the peaks of vinyl methylene (Fig. 1c, peaks labeled a) disappeared and a newly formed methylenepeak (Fig. 1c, peak labeled b,  $\delta 2.25$ ) appeared in the  $^1\text{H-NMR}$  spectra, which indicates the complete reaction of the methacrylate groups of ALG and acrylate groups of peptides.

Photocrosslinked ALG hydrogel disks (diameter=6 mm) were then formed using ALG and ACR-RGD. The gross morphologies of the DMEM or  $\text{diH}_2\text{O}$ -equilibrated ALG and ACR-RGD-ALG hydrogel disks are exhibited in Figure 2a, and their mean diameters were  $6.93 \pm 0.15$  mm and  $7.03 \pm 0.12$  in DMEM, and  $8.27 \pm 0.15$  mm and  $8.20 \pm 0.10$  mm in  $\text{diH}_2\text{O}$ , respectively ( $N=3$ ). While there were no significant differences in gross morphologies or size change between hydrogel with and without ACR-RGD after 24 h equilibration in either solution, hydrogels were significantly larger in  $\text{diH}_2\text{O}$  than in DMEM.

#### Elastic moduli, swelling kinetics, and degradation of the photocrosslinked hydrogels

To compare mechanical properties of photocrosslinked ALG and ACR-RGD-ALG hydrogels, constant strain-rate compression tests were performed over time on samples incubated in DMEM. There was no significant difference in compressive modulus between the two hydrogel groups over the course of 14 days, while the elastic moduli of both hydrogel groups significantly decreased (Fig. 2b). The swelling ratio of the hydrogels was measured over time in DMEM as it reflects changes in their physical and chemical structures. The swelling ratio of both hydrogel conditions significantly decreased over the course of 56 days (Fig. 2c). It

was found that there was no significant difference in swelling ratio between the two hydrogel groups. The mass loss of photocrosslinked hydrogels over time was then determined as a measure of degradation. The mass loss of the photocrosslinked ALG and ACR-RGD-ALG hydrogels was similar in DMEM (Fig. 2d). Both hydrogel conditions lost  $\sim 30\%$  of their mass by 21 days and then exhibited almost complete degradation by 56 days. There was also no significant difference in mass loss between the photocrosslinked ALG and ACR-RGD-ALG hydrogels.

#### hMSC attachment and morphology on the surface of ACR-RGD-ALG hydrogels

hMSCs were seeded onto the surface of photocrosslinked ALG and ACR-RGD-ALG hydrogels to evaluate if the varying of ACR-RGD concentration in hydrogels would affect cell viability, morphology, and adhesion. The viability and morphology of hMSCs on the photocrosslinked hydrogels was examined by fluorescence staining with a Live/Dead assay at days 2 and 5 (Fig. 3a). High cell viability was observed for all hydrogel groups at both time points. The fluorescence photomicrographs also show most of the few hMSCs adherent to the ALG hydrogels and ACR-RGD-ALG hydrogels containing 5 mg ACR-RGD displayed a rounded morphology. In contrast, many hMSCs cultured on the ACR-RGD-ALG hydrogels containing 10 mg ACR-RGD and most of hMSCs cultured on the ACR-RGD-ALG hydrogels containing 20 mg ACR-RGD exhibited a spread morphology at days 2 and 5.

Few hMSCs adhered to the surfaces of ALG and ACR-RGD-ALG containing 5 mg ACR-RGD after 1 day of incubation as demonstrated by DAPI nuclear staining (Fig. 3b). In contrast, a significantly larger number of hMSCs were

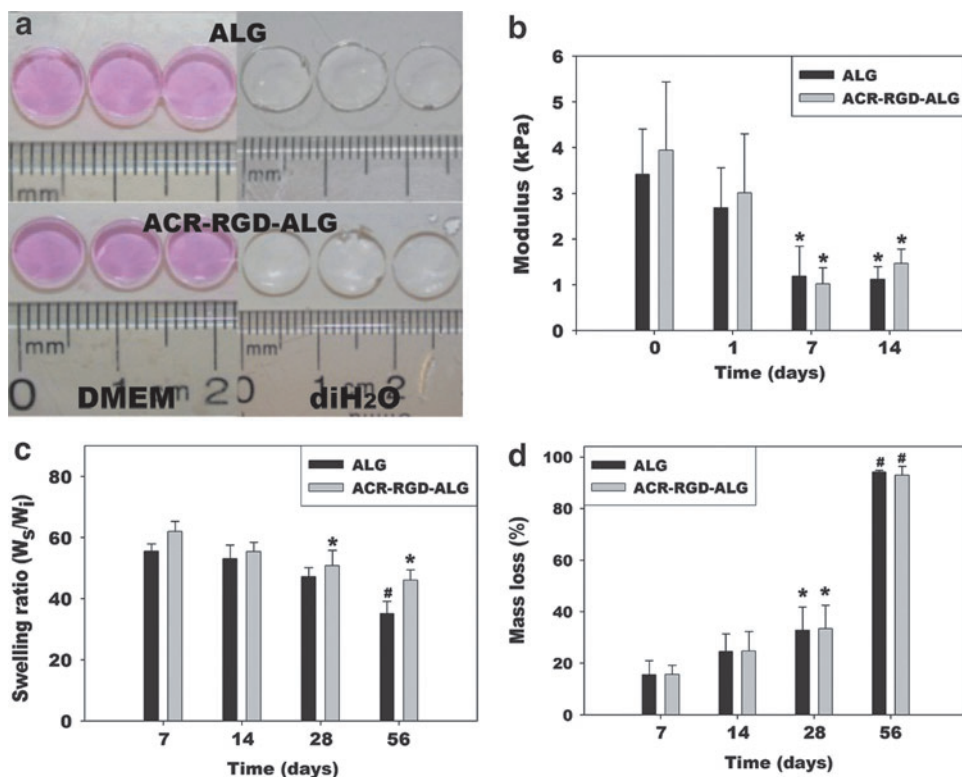


**FIG. 2.** (a) Macroscopic morphology of photocrosslinked ALG and ACR-RGD-ALG (10 mg ACR-RGD/g alginate) hydrogel disks after 24 h equilibration in Dulbecco's modified Eagle medium (DMEM) and deionized water. (b) Elastic moduli in compression. \* $p < 0.05$  compared to Day 0 and 1 within a specific hydrogel group. (c) Swelling ratio in DMEM. \* $p < 0.05$  compared to Day 7 within a specific hydrogel group. # $p < 0.05$  compared to Day 7, 14, and 28 within a specific hydrogel group. (d) *In vitro* degradation in DMEM. \* $p < 0.05$  compared to Day 7 within a specific hydrogel group. # $p < 0.05$  compared to Day 7, 14, and 28 within a specific hydrogel group. Values represent mean  $\pm$  standard deviation ( $N=3$ ). Color images available online at [www.liebertpub.com/tea](http://www.liebertpub.com/tea)

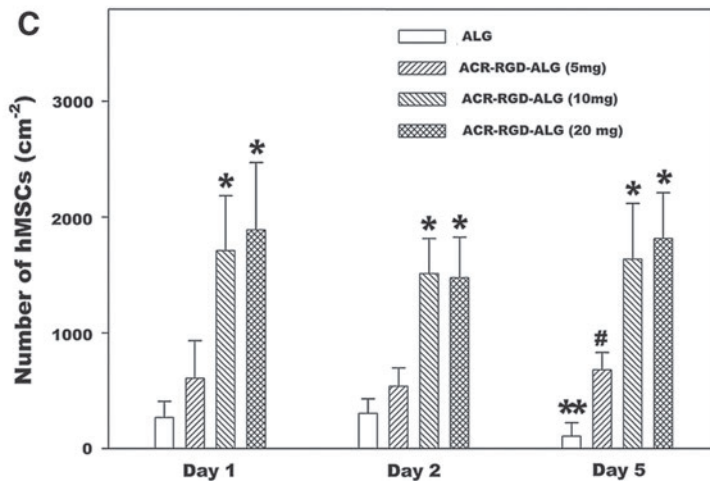
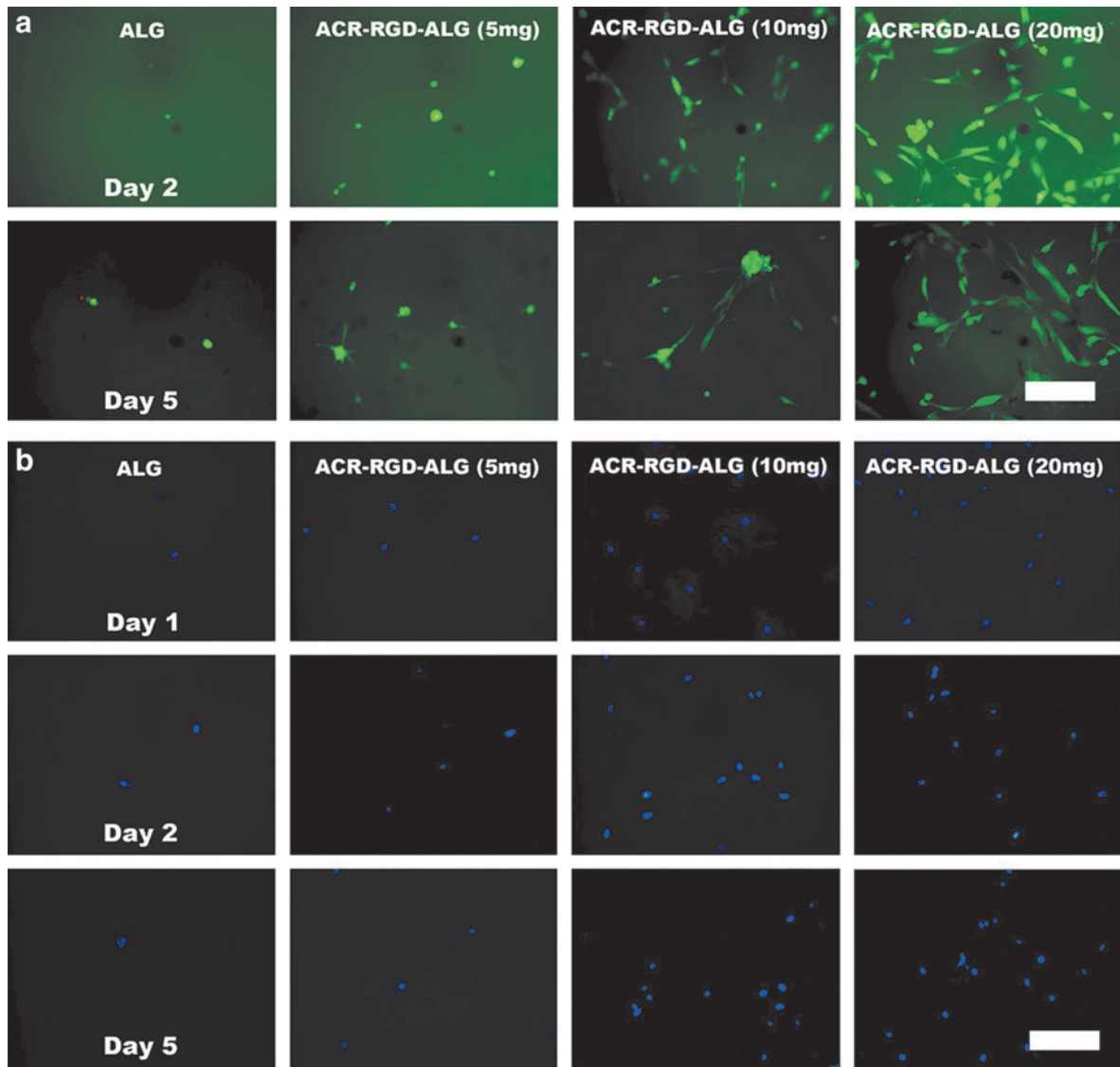


**FIG. 3.** (a) Fluorescence photomicrographs of live (fluorescein diacetate [FDA], green) and dead (ethidium bromide [EB], orange-red) human mesenchymal stem cells (hMSCs) cultured on the surface of photocrosslinked ALG and ACR-RGD-ALG hydrogels for 5 days. (b) Fluorescence photomicrographs of 4',6-diamidino-2-phenylindole (DAPI) positive stained hMSCs after 1, 2, and 5 days culture on the surface of photocrosslinked ALG and ACR-RGD-ALG hydrogels, and (c) quantification of adherent cell number. The scale bars indicate 200  $\mu\text{m}$  and all photographs were taken at the same magnification. \* $p < 0.05$  compared to ALG and ACR-RGD-ALG (5 mg ACR-RGD/g alginate) hydrogels at a specific time point. # $p < 0.05$  compared to the ALG hydrogel at day 5. \*\* $p < 0.05$  compared to ALG hydrogel at days 1 and 2. Values represent mean  $\pm$  standard deviation ( $N = 3$ ). Color images available online at [www.liebertpub.com/tea](http://www.liebertpub.com/tea)

present on the ACR-RGD-ALG hydrogels containing 10 and 20 mg ACR-RGD compared to the ALG hydrogel and the ACR-RGD-ALG hydrogel containing 5 mg ACR-RGD at all time points (Fig. 3c). While the number of adhered hMSCs on the ALG hydrogels without adhesion ligands decreased by 5 days, ACR-RGD-ALG hydrogels supported cell adhesivity for 5 days.

#### hMSC photoencapsulation within ACR-RGD-ALG hydrogels

hMSCs were photoencapsulated within the ALG hydrogels with various amounts of ACR-RGD. The viability of the photoencapsulated hMSCs in the ALG and ACR-RGD-ALG hydrogels was evaluated by Live/Dead assay to examine cell survival during the photoencapsulation and in culture. High cell viability was observed throughout all hydrogel groups at 14 and 28 days (Fig. 4a). To indirectly examine the change in number of the hMSCs encapsulated within the hydrogels, DNA content was measured over a period of 21 days (Fig. 4b). The DNA content of the ALG hydrogels was significantly less compared with all ACR-RGD-ALG hydrogels at

14 days and the 10 and 20 mg ACR-RGD-ALG hydrogels at 21 days, indicating that ACR-RGD incorporation promoted hMSC proliferation in ALG hydrogels. The DNA content within the ACR-RGD-ALG hydrogel groups also significantly increased over the course of 21 days. In contrast, there was no significant increase in the DNA content of ALG hydrogels over time.

#### Discussion

Since cellular behaviors, such as adhesion, spreading, migration, proliferation, and differentiation are influenced by the type,<sup>25</sup> density,<sup>26</sup> and location<sup>27</sup> of cell adhesion ligands, biomaterials have been modified with a variety of such ligands for tissue engineering applications, such as wound healing,<sup>28</sup> osteogenesis,<sup>29</sup> chondrogenesis,<sup>30</sup> adipogenesis<sup>31</sup> and angiogenesis.<sup>32</sup> Given that regulation of cell function in this manner has been demonstrated to be valuable in tissue regeneration strategies, we have developed photocrosslinked ALG hydrogels that permit facile control over the spatial presentation of cell adhesion ligands containing RGD peptide sequences. The results of this study demonstrate that varying

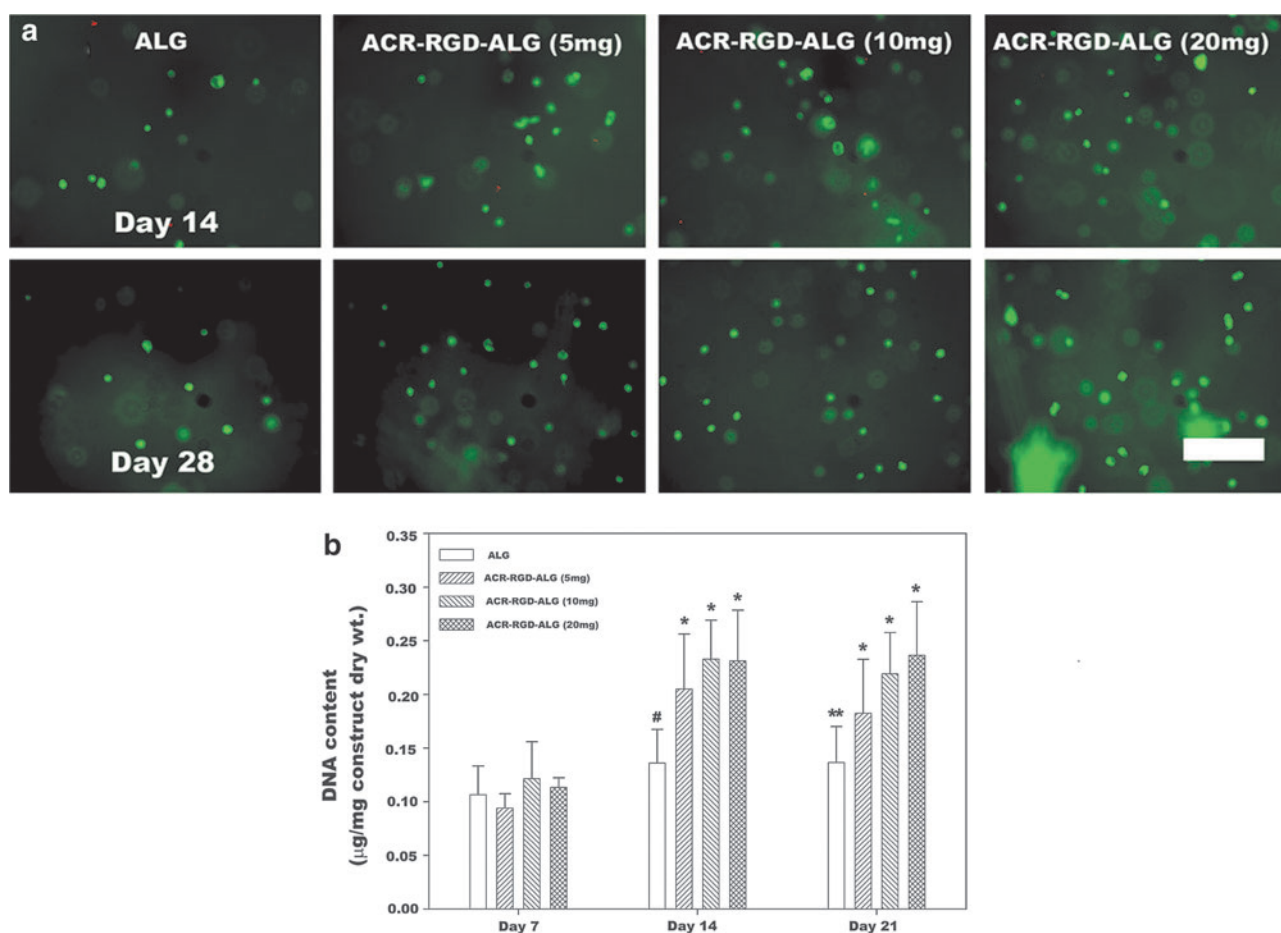


**FIG. 4.** (a) Fluorescence photomicrographs of live (FDA, green) and dead (EB, orange-red) encapsulated hMSCs cultured *in vitro* in the photocrosslinked ALG and ACR-RGD-ALG hydrogels after 14 and 28 days. The scale bar indicates 200  $\mu$ m and all photographs were taken at the same magnification. (b) DNA content in the hMSC/hydrogel constructs normalized to dry weight. \* $p < 0.05$  compared to 7 days. # $p < 0.05$  compared to all ACR-RGD-ALG hydrogels at 14 days. \*\* $p < 0.05$  compared to ACR-RGD-ALG (10 and 20 mg) at 21 days. Values represent mean  $\pm$  standard deviation ( $N = 6-10$ ). Color images available online at [www.liebertpub.com/tea](http://www.liebertpub.com/tea)

the concentration of ACR-RGD in photocrosslinked ALG hydrogels could allow for control over hMSC adhesion, spreading and proliferation without any significant effects on the physical properties of the hydrogels.

Previously, we engineered ALG macromers with RGD-containing cell adhesion ligands using carbodiimide chemistry to create cell adhesive ALG hydrogels after photocrosslinking.<sup>5</sup> However, control over the extent of ligand incorporation in photocrosslinked ALG hydrogels is limited due to the nonlinear relationship between the input and final concentrations of RGD and the low efficiency of RGD modification. In contrast, the method presented in this study resulted in *in situ* RGD modification of ALG hydrogels with high efficiency (~100%) through the photocrosslinking process and provides an easy method to precisely vary the peptide concentration in the resultant hydrogels by varying the concentration of ACR-RGD in the ALG macromer solution. Importantly, unlike chemical modification of ligands directly to the macromer backbone, photocrosslinkable ACR-RGD may also permit fabrication of hydrogels *in situ* with spatial control of ligand presentation and therefore, cell adhesivity. To achieve spatial control over hydrogel cell adhesivity to regulate cell functions, the approach utilized in this study does not require modification of multiple macromer solutions with various ligand concentrations or dilutions with unmodified macromer that result in nonhomogenous ligand spacing.<sup>8</sup>

To use this system to examine the effects of controlled cell adhesivity on cellular behavior as an independent variable, it is important to demonstrate that the adhesion ligand incorporation minimally alters the mechanical properties, swelling ratio, and degradation rate of the hydrogels.<sup>5</sup> Previously, other groups have reported on systems utilizing photocrosslinkable RGD-containing peptides. Mann *et al.* developed an acryloyl-poly(ethylene glycol) (PEG)-RGD for the photopolymerizable PEG hydrogels that allowed for tailorable cell adhesion.<sup>16</sup> Burdick and Anseth also introduced photocrosslinked PEG hydrogels modified with RGD peptide sequences to regulate cell behavior.<sup>23</sup> Similarly, Park *et al.* reported hyaluronic acid hydrogels photofunctionalized with acrylated PEG-RGD created through Michael-type addition chemistry.<sup>21</sup> However, in all of these previous studies the macromer backbones were photofunctionalized with RGD using multifunctional PEGs that may lead to alterations to the hydrogel physical properties<sup>17</sup> and expensive processes for synthesis of chemically active PEG. In contrast, we directly modified the RGD peptides with acrylic acid-NHS without any expensive materials. In addition, the ALG and ACR-RGD-ALG hydrogels exhibited similar physical properties over time. Since these properties reflect on the cross-linked structure of the hydrogels,<sup>33</sup> these results indicate that ACR-RGD incorporation into ALG hydrogels does not substantially affect their macromolecular structure over time.

This biomaterials system could prove useful when combined with high-throughput technologies, which have recently emerged as a valuable tool, to investigate the role of multiple different microenvironmental signals, such as cell-extracellular matrix (ECM) interactions and soluble growth factors, individually and in combination, on cell function.<sup>34-37</sup> For example, microarrays of small molecules and peptides have been developed to miniaturize assays and enable screening of large libraries of cell adhesion molecules.<sup>35</sup> As a result, this technology has been used to enable

high-throughput screening studies for examining cell adhesivity signaling resulting from these cell-material interactions using immunofluorescence assays. Alternatively, Acharya *et al.* utilized a surface gradient platform with the RGD peptide as a high-throughput system to investigate the relationship between adhesion ligand concentration and dendritic cell adhesion and function.<sup>37</sup> Flaim *et al.* created ECM microarrays to identify combinations of ECM molecules that would synergistically enhance stem cell differentiation.<sup>38</sup> Since the acrylated peptides can easily be integrated into photocrosslinkable biomaterial systems, a variety of acrylated peptide types, concentrations and combinations could potentially be used with existing high-throughput technologies to investigate the influence of these variables on cell behavior on or within 3D hydrogel systems. This could be a powerful tool for understanding and optimization of cell-materials interactions.

## Conclusion

We have engineered a photocrosslinkable and biodegradable ALG hydrogel with easily controllable cell adhesivity by incorporation of ACR-RGD. Photocrosslinked ALG and ACR-RGD-ALG hydrogels exhibited similar mechanical properties, swelling ratios, and degradation rate over time, showing that the addition of the cell adhesion ligands does not affect hydrogel physical properties. ACR-RGD incorporation into ALG hydrogels promoted hMSC adhesion and spreading on the surface of the hydrogels, whereas minimal adhesion was supported on the ALG hydrogels. In addition, hMSCs could be easily encapsulated with the ACR-RGD-ALG hydrogels via suspension followed by *in situ* photopolymerization in a macromer solution of ALG and ACR-RGD, and were able to proliferate in these hydrogels. The photocrosslinked ACR-RGD-ALG hydrogels developed in this study may allow for simpler spatial control over the hydrogels' cell adhesive properties and find great utility in understanding cell-biomaterial interactions, high-throughput technologies and tissue engineering.

## Acknowledgments

The authors thank Caitlin Powell for research assistance, and Dr. Arnold Caplan's Skeletal Research Center Mesenchymal Stem Cell facility, especially Dr. Donald Lennon and Ms. Margie Harris, for providing the hMSCs. The authors gratefully acknowledge funding from the National Institutes of Health (AR063194, DE022376, AR061265), the Department of Defense Congressionally Directed Medical Research Programs (OR110196), the AO Foundation, and a New Scholar in Aging grant from the Ellison Medical Foundation.

## Disclosure Statement

The authors have no conflicts of interest.

## References

1. Jeon, O., Bouhadir, K.H., Mansour, J.M., and Alsberg, E. Photocrosslinked alginate hydrogels with tunable biodegradation rates and mechanical properties. *Biomaterials* **30**, 2724, 2009.
2. Jeon, O., Alt, D.S., Ahmed, S.M., and Alsberg, E. The effect of oxidation on the degradation of photocrosslinkable alginate hydrogels. *Biomaterials* **33**, 3503, 2012.

3. Rowley, J.A., Madlambayan, G., and Mooney, D.J. Alginate hydrogels as synthetic extracellular matrix materials. *Biomaterials* **20**, 45, 1999.
4. Smetana, K. Cell biology of hydrogels. *Biomaterials* **14**, 1046, 1993.
5. Jeon, O., Powell, C., Ahmed, S.M., and Alsberg, E. Biodegradable, photocrosslinked alginate hydrogels with independently tailorable physical properties and cell adhesivity. *Tissue Eng Part A* **16**, 2915, 2010.
6. Jeon, O., Powell, C., Solorio, L., Krebs, M.D., and Alsberg, E. Affinity-based growth factor delivery using biodegradable, photocrosslinked heparin-alginate hydrogels. *J Control Release* **154**, 258, 2011.
7. Mann, M., Ong, S.E., Gronborg, M., Steen, H., Jensen, O.N., and Pandey, A. Analysis of protein phosphorylation using mass spectrometry: deciphering the phosphoproteome. *Trends Biotechnol* **20**, 261, 2002.
8. Lee, K.Y., Alsberg, E., Hsiong, S., Comisar, W., Linderman, J., Ziff, R., and Mooney, D. Nanoscale adhesion ligand organization regulates osteoblast proliferation and differentiation. *Nano Lett* **4**, 1501, 2004.
9. Gomez, N., and Schmidt, C.E. Nerve growth factor-immobilized polypyrrole: bioactive electrically conducting polymer for enhanced neurite extension. *J Biomed Mater Res A* **81**, 135, 2007.
10. Onuki, Y., Nishikawa, M., Morishita, M., and Takayama, K. Development of photocrosslinked polyacrylic acid hydrogel as an adhesive for dermatological patches: involvement of formulation factors in physical properties and pharmacological effects. *Int J Pharm* **349**, 47, 2008.
11. Moon, J.J., Lee, S.H., and West, J.L. Synthetic biomimetic hydrogels incorporated with Ephrin-A1 for therapeutic angiogenesis. *Biomacromolecules* **8**, 42, 2007.
12. Suri, S., Singh, A., and Schmidt, C.E. Photofunctionalization of materials to promote protein and cell interactions for tissue-engineering applications. In: Puleo, D.A., and Bizios, R., eds. *Biological Interactions on Materials Surfaces*. New York: Springer US; 2009. pp. 297.
13. Halstenberg, S., Panitch, A., Rizzi, S., Hall, H., and Hubbell, J.A. Biologically engineered protein-graft-poly(ethylene glycol) hydrogels: a cell adhesive and plasmin-degradable biosynthetic material for tissue repair. *Biomacromolecules* **3**, 710, 2002.
14. Rydholm, A.E., Held, N.L., Benoit, D.S.W., Bowman, C.N., and Anseth, K.S. Modifying network chemistry in thiol-acrylate photopolymers through postpolymerization functionalization to control cell-material interactions. *J Biomed Mater Res Part A* **86A**, 23, 2008.
15. Liu, B., Lewis, A.K., and Shen, W. Physical hydrogels photo-cross-linked from self-assembled macromers for potential use in tissue engineering. *Biomacromolecules* **10**, 3182, 2009.
16. Mann, B.K., Gobin, A.S., Tsai, A.T., Schmedlen, R.H., and West, J.L. Smooth muscle cell growth in photopolymerized hydrogels with cell adhesive and proteolytically degradable domains: synthetic ECM analogs for tissue engineering. *Biomaterials* **22**, 3045, 2001.
17. Zustiak, S.P., and Leach, J.B. Hydrolytically degradable poly(ethylene glycol) hydrogel scaffolds with tunable degradation and mechanical properties. *Biomacromolecules* **11**, 1348, 2010.
18. Hahn, M.S., Miller, J.S., and West, J.L. Three-dimensional biochemical and biomechanical patterning of hydrogels for guiding cell behavior. *Adv Mater* **18**, 2679, 2006.
19. Hern, D.L., and Hubbell, J.A. Incorporation of adhesion peptides into nonadhesive hydrogels useful for tissue resurfacing. *J Biomed Mater Res* **39**, 266, 1998.
20. Seidlits, S.K., Drinnan, C.T., Petersen, R.R., Shear, J.B., Suggs, L.J., and Schmidt, C.E. Fibronectin-hyaluronic acid composite hydrogels for three-dimensional endothelial cell culture. *Acta Biomater* **7**, 2401, 2011.
21. Park, Y.D., Tirelli, N., and Hubbell, J.A. Photopolymerized hyaluronic acid-based hydrogels and interpenetrating networks. *Biomaterials* **24**, 893, 2003.
22. He, X.Z., Ma, J.Y., and Jabbari, E. Effect of grafting RGD and BMP-2 protein-derived peptides to a hydrogel substrate on osteogenic differentiation of marrow stromal cells. *Langmuir* **24**, 12508, 2008.
23. Burdick, J.A., and Anseth, K.S. Photoencapsulation of osteoblasts in injectable RGD-modified PEG hydrogels for bone tissue engineering. *Biomaterials* **23**, 4315, 2002.
24. Lennon, D.P., Haynesworth, S.E., Bruder, S.P., Jaiswal, N., and Caplan, A.I. Human and animal mesenchymal progenitor cells from bone marrow: identification of serum for optimal selection and proliferation. *In Vitro Cell Dev Biol* **32**, 602, 1996.
25. Mochizuki, M., Yamagata, N., Philp, D., Hozumi, K., Watanabe, T., Kikkawa, Y., Kadoya, Y., Kleinman, H.K., and Nomizu, M. Integrin-dependent cell behavior on ECM peptide-conjugated chitosan membranes. *Biopolymers* **88**, 122, 2007.
26. Rowley, J.A., and Mooney, D.J. Alginate type and RGD density control myoblast phenotype. *J Biomed Mater Res* **60**, 217, 2002.
27. Cavalcanti-Adam, E.A., Aydin, D., Hirschfeld-Warneken, V.C., and Spatz, J.P. Cell adhesion and response to synthetic nanopatterned environments by steering receptor clustering and spatial location. *HFSP J* **2**, 276, 2008.
28. Kishida, A., Takatsuka, M., and Matsuda, T. RGD-albumin conjugate: expression of tissue regeneration activity. *Biomaterials* **13**, 924, 1992.
29. Hsiong, S.X., Boonthekul, T., Huebsch, N., and Mooney, D.J. Cyclic arginine-glycine-aspartate peptides enhance three-dimensional stem cell osteogenic differentiation. *Tissue Eng Part A* **15**, 263, 2009.
30. Re'em, T., Tsur-Gang, O., and Cohen, S. The effect of immobilized RGD peptide in macroporous alginate scaffolds on TGFbeta1-induced chondrogenesis of human mesenchymal stem cells. *Biomaterials* **31**, 6746, 2010.
31. Kang, S.W., Cha, B.H., Park, H., Park, K.S., Lee, K.Y., and Lee, S.H. The effect of conjugating RGD into 3D alginate hydrogels on adipogenic differentiation of human adipose-derived stromal cells. *Macromol Biosci* **11**, 673, 2011.
32. Yu, J., Gu, Y., Du, K.T., Mihardja, S., Sievers, R.E., and Lee, R.J. The effect of injected RGD modified alginate on angiogenesis and left ventricular function in a chronic rat infarct model. *Biomaterials* **30**, 751, 2009.
33. Pillay, V., and Fasshi, R. *In vitro* release modulation from crosslinked pellets for site-specific drug delivery to the gastrointestinal tract. II. Physicochemical characterization of calcium-alginate, calcium-pectinate and calcium-alginate-pectinate pellets. *J Control Release* **59**, 243, 1999.
34. Yang, F., Mei, Y., Langer, R., and Anderson, D.G. High throughput optimization of stem cell microenvironments. *Comb Chem High Throughput Screen* **12**, 554, 2009.
35. Falsey, J.R., Renil, M., Park, S., Li, S.J., and Lam, K.S. Peptide and small molecule microarray for high throughput cell adhesion and functional assays. *Bioconjug Chem* **12**, 346, 2001.



36. Gallego-Perez, D., Higuera-Castro, N., Sharma, S., Reen, R.K., Palmer, A.F., Gooch, K.J., Lee, L.J., Lannutti, J.J., and Hansford, D.J. High throughput assembly of spatially controlled 3D cell clusters on a micro/nanoplatfrom. *Lab Chip* **10**, 775, 2010.
37. Acharya, A.P., Dolgova, N.V., Moore, N.M., Xia, C.Q., Clare-Salzler, M.J., Becker, M.L., Gallant, N.D., and Keselowsky, B.G. The modulation of dendritic cell integrin binding and activation by RGD-peptide density gradient substrates. *Biomaterials* **31**, 7444, 2010.
38. Flaim, C.J., Chien, S., and Bhatia, S.N. An extracellular matrix microarray for probing cellular differentiation. *Nat Methods* **2**, 119, 2005.

Address correspondence to:

*Eben Alsberg, PhD*

*Department of Biomedical Engineering*

*Case Western Reserve University*

*10900 Euclid Ave.*

*Cleveland, OH 44106*

*E-mail: eben.alsberg@case.edu*

*Received: September 25, 2012*

*Accepted: January 16, 2013*

*Online Publication Date: February 25, 2013*